ELSEVIER

International Journal of Fatigue 23 (2001) 565–573

International Journal of Fatigue

www.elsevier.com/locate/ijfatigue

Fatigue properties of Al–1Mg–0.6Si foam at low and ultrasonic frequencies

B. Zettl *, H. Mayer, S.E. Stanzl-Tschegg

Institute of Meteorology and Physics, University of Agricultural Sciences, Tuerkenschanzstr 18, A-1180 Vienna, Austria

Received 30 November 2000; received in revised form 12 March 2001; accepted 15 March 2001

Abstract

The fatigue properties of Al–1wt%Mg–0.6wt%Si aluminium foam were investigated at 1–10 Hz with a servohydraulic fatigue testing machine and at 20 kHz using ultrasonic equipment. Foamed rods were cycled at constant amplitude under fully reversed loading conditions. Within the ranges of scatter, lifetimes measured at both frequencies are similar. The foam shows an endurance limit, and specimens either fail below approximately 10^7 cycles or they survive for 10^9 cycles or more. A probability of 50% for fracture (mean endurance limit) was found at $\Delta\varepsilon/2=0.32\times10^{-3}$ (1.31 MPa). Fatigue cracks initiate in the interior closed cell structure at holes or pre-existing cracks in the cell walls or in areas where the cell walls are thin, and the surface layer cracks in the following. At the endurance limit, fatigue cracks may initiate in cell walls, however, they are trapped at nodes of cells.

Keywords: Aluminium foam; Fatigue; Lifetime; Endurance limit; Ultrasonic testing

1. Introduction

Aluminium foams have received increased attention as a potential structural material in the transportation industry [1]. The characteristic deformation behaviour of foams under compression forces, namely the formation of a plateau-like regime in the stress–strain curve, where compression forces remain nearly constant over a wide range of plastic deformations, makes them appropriate for use as crash energy absorbing elements [2]. Additionally, several multi-functional construction elements in vehicles (sound absorption, heat dissipation, etc.) can be realized with aluminium foams due to a low mass-density and a high specific stiffness [3].

Structural components of vehicles are frequently subjected to varying loads due to numerous reasons (driving forces, road conditions, engine vibrations, etc.). Such cyclic stresses may cause fatigue damage, and knowledge of the cyclic properties of potential materials for the transportation industry is therefore of great interest. Fatigue investigations of metallic foams mainly concentrate on cyclic compression loads, rather high cyclic stresses and cycles to failure below 10^6 [4–9], whereas high-cycle-fatigue studies are rare [10]. However, numbers of load cycles of the order of 10^8 or more may be imposed on load-bearing car components, for example, and fatigue data at high as well as low numbers of cycles to failure are necessary for an appropriate design. Additionally, cyclic compression loading is a rather unrealistic simulation of in-service conditions of a component, which will be more probably subjected to bending forces or vibrations. In the present investigation, cyclic properties are investigated under fully reversed loading conditions. Besides fatigue experiments in the low cycle regime, several specimens loaded with 10^9 cycles or more served to investigate the cyclic properties at very high numbers of cycles.

Using conventional fatigue testing equipment, cyclic loading of a specimen in the very high cycle regime requires long testing times, and several specimens have to be tested to obtain statistically significant data of inhomogeneous materials, like metallic foams. A time-saving method to investigate high cycle fatigue properties of materials is the ultrasonic fatigue testing method, where the specimens are loaded with cyclic frequencies

* Corresponding author. Tel.: +43-1-470-5820-10; fax: +43-1-470-5820-60.

E-mail address: bernd.zettl@mail.boku.ac.at (B. Zettl).

0142-1123/01/$ - see front matter
PII: S0142-1123(01)00025-1

of approximately 20 kHz. However, this experimental procedure, although successfully used to investigate the fatigue properties of bulk or composite materials, has not been used to investigate foams until now [11]. It is therefore necessary to prove that the fatigue properties of aluminium foam determined with the ultrasonic method are similar to the results obtained at low frequency with conventional fatigue testing equipment.

Fatigue lifetimes of foams are frequently presented using stress amplitudes in the literature, and the stress amplitude is defined as the ratio of applied (tension or compression) force to the cross section area of the foamed structure. However, in ultrasonic fatigue experiments the cyclic strain can be measured, whereas knowledge of the stress–strain behaviour of a material is necessary to determine the cyclic stresses. In the elastic regime, cyclic stresses can be calculated using the Young's modulus of a specimen. In contrast to bulk polycrystalline metallic material, the elastic constants of foams are not only related to the type of material, but the structure and the density of a specimen additionally influences its stiffness. Young's moduli of several specimens were determined with two different methods, i.e. evaluating the stress–strain behaviour and using a dynamic resonance method. Static experiments served to evaluate the onset of plastic deformation under tension and compression forces.

2. Material

The aluminium foam was produced from powder metallurgical prepared precursor material with entrapped titanium hydride as the foaming agent. Chemical composition of the investigated foam is Al–1wt%Mg–0.6wt%Si (AlMg1Si0.6). The commercial name of the material is Alulight®. The material was produced as rods of 160 mm length and of 17 mm diameter. The rods consist of a continuous surface layer with a thickness of about 0.5 mm and a closed cell structure inside. Three typical cross sections of foamed rods are shown in Fig. 1. A quantitative image analysis [12] showed that most frequent cell diameters are about 1 mm. Cells with a diameter of about 3–4 mm occupy the largest cross section area, and the largest cell diameters were 8–9 mm. The density of the material is 0.56 ± 0.12 kg/dm^3. One series of specimens has been tested as fabricated. Another series of specimens has been artificially aged before testing (aged at 160°C for 14 h).

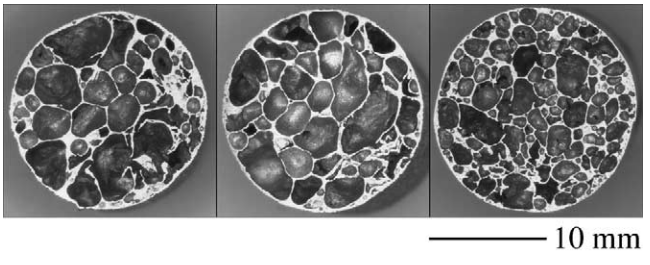

Fig. 1. Typical cross sections of foamed rods with different mean cell sizes; coarse structures (right) and fine structures (left).

3. Procedure

3.1. Fatigue tests with servohydraulic equipment

A servohydraulic fatigue testing equipment served to determine the fatigue properties of AlMg1Si0.6-foam at conventional cyclic frequencies under fully reversed loading conditions. Specimens with a length of approximately 60 mm (Fig. 2) were loaded with a constant cyclic force, and force amplitude as well as mean force were kept constant during the tests. Cycling frequency was 1 Hz until 10^4 cycles were reached and 10 Hz afterwards.

The cyclic strain amplitude at the beginning of fatigue loading, $\Delta\varepsilon/2$, serves as a measure for the magnitude of loading and to compare fatigue lifetimes at high and low frequencies. $\Delta\varepsilon/2$ was measured using two strain gauges (measuring area 10 mm×5 mm) attached to the surfaces of the specimens (as shown in Fig. 2). With these (relatively large) strain gauges it is possible to obtain a representative value of the cyclic strain of a specimen. Typically, cyclic strains measured with this technique at different places of a specimen coincided within 5–10%.

Cyclic force, cyclic strain amplitude and displacement of hydraulic piston were monitored during the experiments. When a crack initiates, the compliance of the

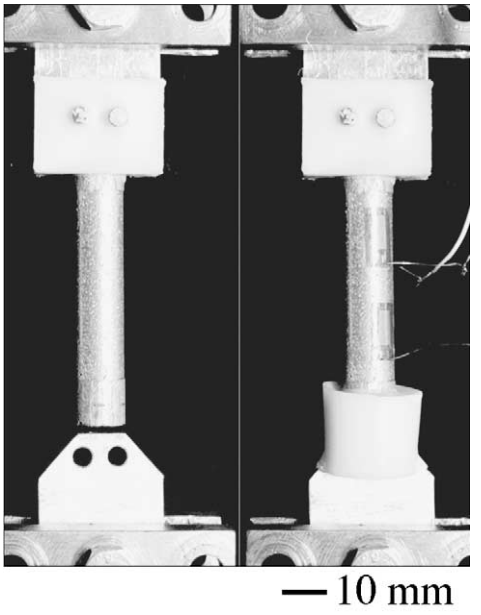

Fig. 2. Specimen used for fatigue tests in servohydraulic equipment. Epoxy resin at both ends of the specimen serves to eliminate undesirable bending stresses. Strain amplitude is measured with strain gauges.

specimens increases, and monitoring of the displacement of the hydraulic piston can be correlated to specimen failure.

3.2. Fatigue tests with ultrasonic equipment

In ultrasonic fatigue experiments, specimens were subjected to a fully reversed tension–compression resonance loading at a cyclic frequency of approximately 20 kHz. The amplitude of the vibration of the specimen was measured using an electromagnetic displacement gauge located at one end of the specimen and was kept constant during the test.

The lengths of all vibrating mechanical parts of the load train (ultrasonic transducer, ultrasonic horn and specimen) were adjusted to vibrate in resonance to obtain large enough load amplitudes to fracture the specimens. Initiation of a fatigue crack in the specimen leads to an increase of the specimen's compliance and thus to a decrease in the frequency of resonance vibration. Control of loading frequency keeps ultrasonic vibration in resonance. A frequency limit was used to stop the test, if the specimen failed. Specimens were cycled until failure or to a minimum of 10^9 cycles if the specimen did not fail. To avoid heating of the specimens, they were loaded in a pulse–pause sequence. After pulses of 1000 load cycles each periodic pauses of adequate length (25–200 ms) served to cool the specimens and to keep the specimens' temperatures below 25°C. Details of control and evaluation of ultrasonic fatigue experiments are described elsewhere [11].

The specimen length, l is half of the acoustic wavelength, λ of a tension–compression wave at a frequency, f of 20 kHz. The resonance length of a foamed specimen with Young's modulus E and mass density ρ is therefore:

$$l=\frac{\lambda}{2}=\frac{1}{2f}\sqrt{\frac{E}{\rho}} \quad (1)$$

This means that specimen length would be approximately 67 mm. However, for proper reflection of the acoustic waves, an aluminium disc was attached with an adhesive at one end of the specimen. This additional mass reduces the length of the specimens to typically 50 mm. At the other end a thread serves to mount the specimen. Fig. 3 shows a specimen used in ultrasonic fatigue tests.

The vibration amplitude varies sinusoidally along the length of the specimens and becomes maximal at both ends. The strain amplitude is the derivative of the vibration amplitude. It becomes maximal at the places of the vibration nodes, i.e. in the centre of the specimens and decreases sinusoidally towards both ends of the specimens. Within a distance of 7.5 mm from the centre of the specimens, the decrease of cyclic strain amplitude is less than 10%.

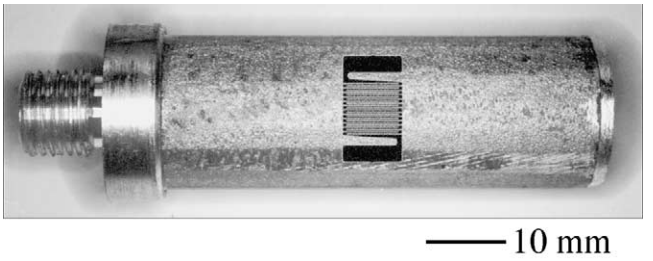

Fig. 3. Specimen used for ultrasonic fatigue tests. The specimen consists of a foamed rod, a disc to reflect ultrasonic waves (right) and thread (left). Two strain gauges (in the centre, back- and foreside) are used to monitor the cyclic strain.

The cyclic strain amplitude, $\Delta\varepsilon/2$, serves as a measure for the magnitude of the cyclic load. Cyclic strain amplitudes were measured with strain gauges, which served to calibrate the experiments and to monitor cyclic loading during the tests. Due to the rather inhomogeneous structure of the foam, relatively large strain gauges with a measuring area of 6 mm×6 mm (which is larger than the medium cell sizes) were used to determine the cyclic strain amplitude. With these strain gauges, strain amplitudes measured at different places in the centre of the specimens coincide within typically 5–10%.

To calculate the cyclic stress in ultrasonic experiments, Young's modulus of the foamed rods has to be known. To obtain this parameter with high frequency equipment, the following procedure was used: foamed rods of about 25 cm length in acoustic contact with the ultrasonic transducer were stimulated to longitudinal vibrations, and stimulation frequencies were adjusted to obtain resonance. Several vibration maxima and vibration nodes appear along the length of the rods. The distances of two vibration nodes were measured with an electromagnetic displacement gauge and served to determine the Young's moduli according to Eq. (1).

4. Results

4.1. Lifetimes versus cyclic strain amplitudes

In Fig. 4, results of endurance tests obtained with servohydraulic equipment are shown with full symbols. Cyclic strain amplitudes at the beginning of constant force amplitude loading range from $\Delta\varepsilon/2=0.4\times10^{-3}$ to 1.1×10^{-3}, and cycles to failure were measured between 20 and 6×10^6. Triangles and circles represent lifetimes of Al–1Mg–0.6Si foam with and without artificial aging. Within the range of scatter, lifetimes of heat-treated and as-produced specimens are similar. The straight lines approximate the fatigue data assuming a power-law dependence of cyclic strain amplitudes, $\Delta\varepsilon/2$ and numbers of cycles to failure, N:

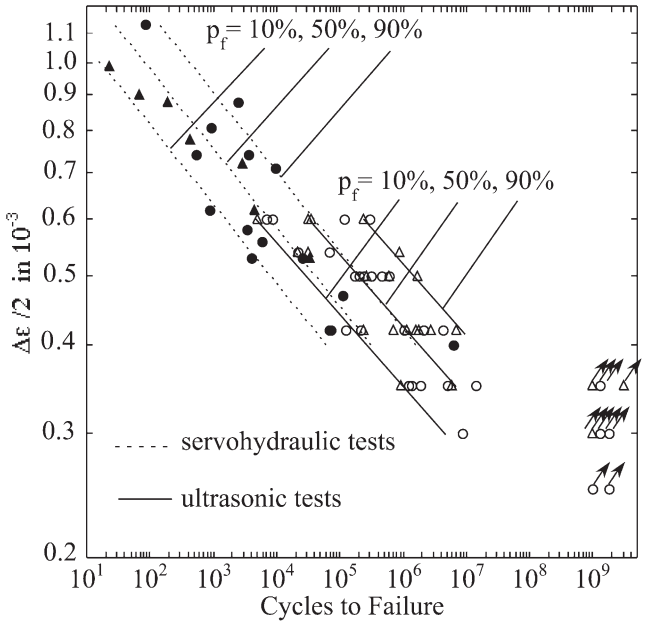

Fig. 4. Fatigue data of AlSi1Mg0.6 foam without heat treatment (cycles) and after artificial aging (triangles). Full symbols represent data obtained at 1–10 Hz and open symbols data obtained at 20 kHz. Lines indicate a fracture probability of 10, 50 and 90%. Lifetimes are presented versus the cyclic strain amplitude. $\Delta\varepsilon/2$ refers to the strain amplitude at the beginning of fatigue cycling.

$$N^n.\left(\frac{\Delta\varepsilon}{2}\right)=\text{const.} \quad (2)$$

The exponent n in Eq. (2) is 0.112 in low frequency tests. Assuming a Gaussian distribution of logarithmics of cycles to failure, parallel dashed lines indicate a probability of failure of 10 and 90%, respectively.

Fatigue data obtained with ultrasonic fatigue testing equipment are shown with open symbols in Fig. 4, and solid lines indicate failure probabilities of 10, 50 and 90%, respectively. Runouts are marked with an arrow. Exponent n of the approximation function in high frequency experiments is 0.102. The investigated cyclic strain amplitudes, $\Delta\varepsilon/2$ range from 0.25×10^{-3} to 0.6×10^{-3}, and specimens failed at numbers of cycles between 7×10^3 and 1.37×10^7. Specimens which did not fail within this range, also survived 10^9 cycles or more. This means, that Al–1Mg–0.6Si foam exhibits an endurance limit. A probability of 50% for fracture (mean endurance limit) is found at a cyclic strain amplitude of 0.32×10^{-3}.

4.2. Lifetimes versus cyclic stress amplitudes

Cyclic stress amplitude, i.e. ratio of cyclic force and geometric cross section area in servohydraulic experiments, may be used as an alternative measure to characterize the magnitude of loading. In ultrasonic frequency experiments, cyclic stress may be calculated according to Hooke's law using the measured cyclic strain amplitude and the Young's modulus of the specimen, if loading is in the linear elastic regime. An evaluation of the elastic–plastic deformation of two specimens served to determine the maximum strain amplitude, where deformation of the foam may be recognized as (nearly) elastic.

A specimen with a length of 60 mm was deformed with a constant piston displacement of 0.01 mm/s under tension forces, and another specimen was loaded similarly under compression forces. Fig. 5 shows the tension and compression force and stress versus the average strain (i.e. ratio of elongation and initial specimen length) of both specimens. The deformation of the specimen loaded with tension forces showed a nearly elastic deformation (plastic strain below 10^{-4}) for tension forces below 1080 N (average strain: 4.8 MPa). Compressive forces below 544 N (average strain: 2.4 MPa) lead to nearly elastic deformation of the specimen in the compressive test. This means that cyclic stresses in ultrasonic fatigue experiments at strain amplitudes below maximum 0.6×10^{-3} may be calculated with reasonable accuracy assuming linear elastic cycling.

The elastic deformation of 20 specimens tested with the servohydraulic equipment served to determine the Young's moduli, and Fig. 6 shows a classification of the obtained results. The average value is 4.3±0.7 GPa. Nineteen specimens served to determine the Young's moduli with the dynamic method, and a value of 3.9±0.7 GPa was found. Scatter of data obtained with both testing procedures is relatively large. Within this scatter, however, no statistically significant difference of the Young's moduli determined with the static and the dynamic method exists. Stiffness of the foamed rods may be mainly attributed to the continuous surface layer. If the surface layers of four specimens were removed, Young's modulus decreased to 2.5±0.4 GPa.

In Fig. 7 results of low and high frequency fatigue tests are plotted versus the cyclic stress amplitude. To

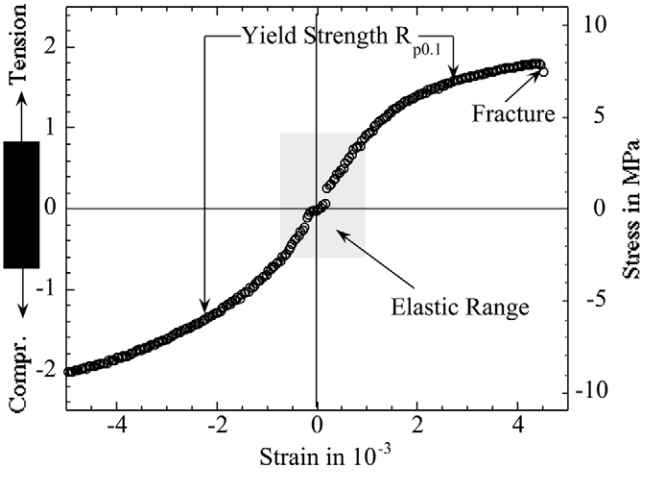

Fig. 5. Stress–strain curve of a specimen subjected to tension forces and of a specimen loaded with compression forces.

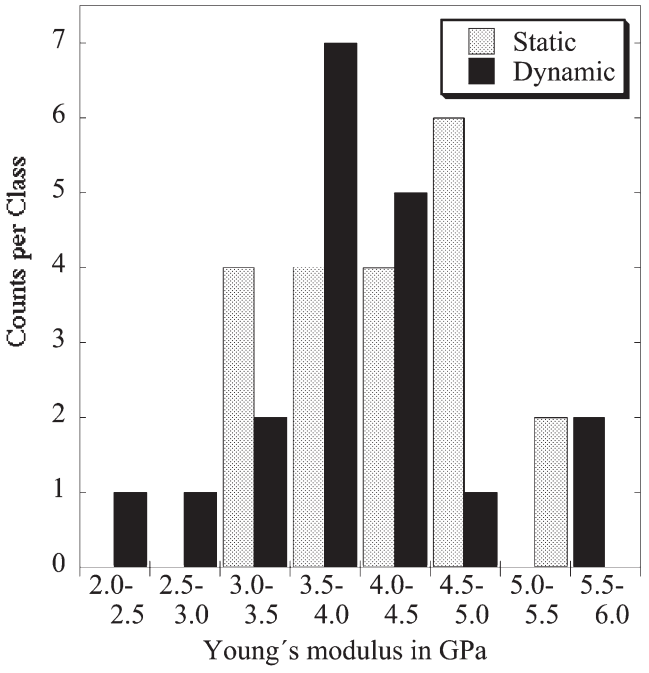

Fig. 6. Young's modulus of AlSi1Mg0.6 foam determined with servohydraulic experiments (static) and from resonance vibration experiments at 20 Hz (dynamic).

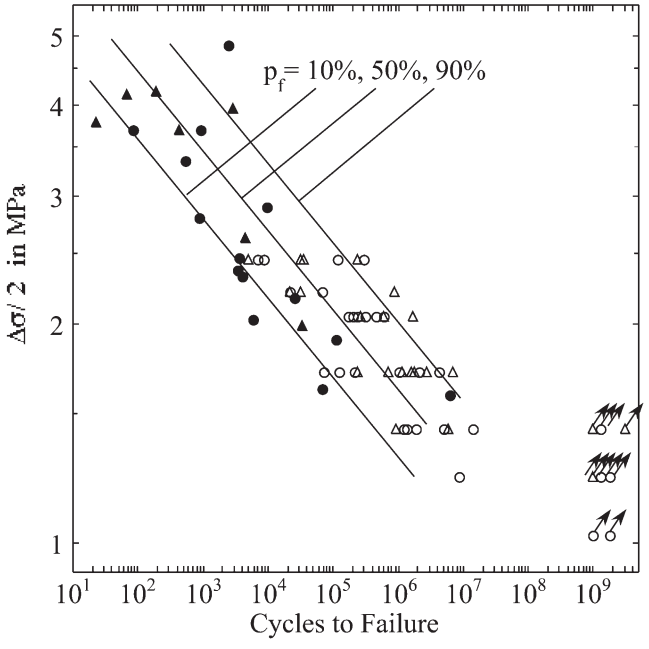

Fig. 7. Fatigue data of AlSi1Mg0.6 foam presented versus the cyclic stress amplitude. For symbols refer to Fig. 4.

calculate cyclic stresses in high frequency experiments, a Young's modulus of 4.1 GPa (which is the average value obtained with the low and the high frequency methods) was used. In Fig. 7, lines indicating different probabilities of failure were determined using both low and high frequency experiments.

4.3. Localization of crack initiation

4.3.1. Compliance measurements

The initiation of fatigue cracks leads to an increase of specimen compliance. In servohydraulic experiments under constant cyclic force, motion of hydraulic ram increases and in ultrasonic fatigue experiments, frequency of resonance vibration decreases. Fig. 8(a) shows the increase of ram displacement amplitude in servohydraulic fatigue tests. Load cycles are normalized with respect to number of cycles to failure. Similarly, Fig. 8(b) shows the decrease of resonance frequency during high frequency experiments. Below approximately 60% of the lifetime of a specimen, ram displacement amplitudes do not show a significant increase in the specimen compliance. However, cyclic resonance frequency is a more sensitive measure of the specimen's compliance than ram displacement. During approximately the first 60% of the lifetime of a specimen, a slight decrease in resonance frequency indicates the evolution of fatigue damage. Both piston displacement and resonance frequencies indicate a pronounced increase of specimen compliance after typically 60–80% of the fatigue lifetime. A microscopical investigation of specimen surfaces did not show a fatigue crack in the surface layer, until about 80% of the lifetime has been reached. This means that fatigue cracks preferentially initiate in the interior of a foamed rod. The continuous surface layer contributes significantly to the stiffness of the rod, and compliance rapidly increases therefore when cracks start to grow in the surface layer.

4.3.2. Lifetime measurements of specimens without surface layer

To determine the fatigue properties of the closed cell foam structure in the interior of the rods, the surface layers of seven specimens have been removed. In Fig. 9 lifetimes of specimens with and without surface layers are compared. Full and open rhombohedra represent specimens without surface layer tested at conventional and ultrasonic frequency, respectively. Within the relatively large scatter of fatigue data, lifetimes of specimens with and without surface layers are similar, if data are presented versus the cyclic strain amplitude.

4.3.3. Mass density at the place of crack initiation

Depending on the internal foam structure and the thickness of the surface layer, the density of foamed rods varies along their length. To correlate the local material density to preferential crack initiation places, small slices with a length of typically 6 mm were cut at the place where a fatigue crack caused final fracture. In Fig. 10 mass density of these slices is shown with respect to the mass densities of the respective specimens. A tendency is visible that fatal cracks mainly occur at places of low material density. However, the relative value is

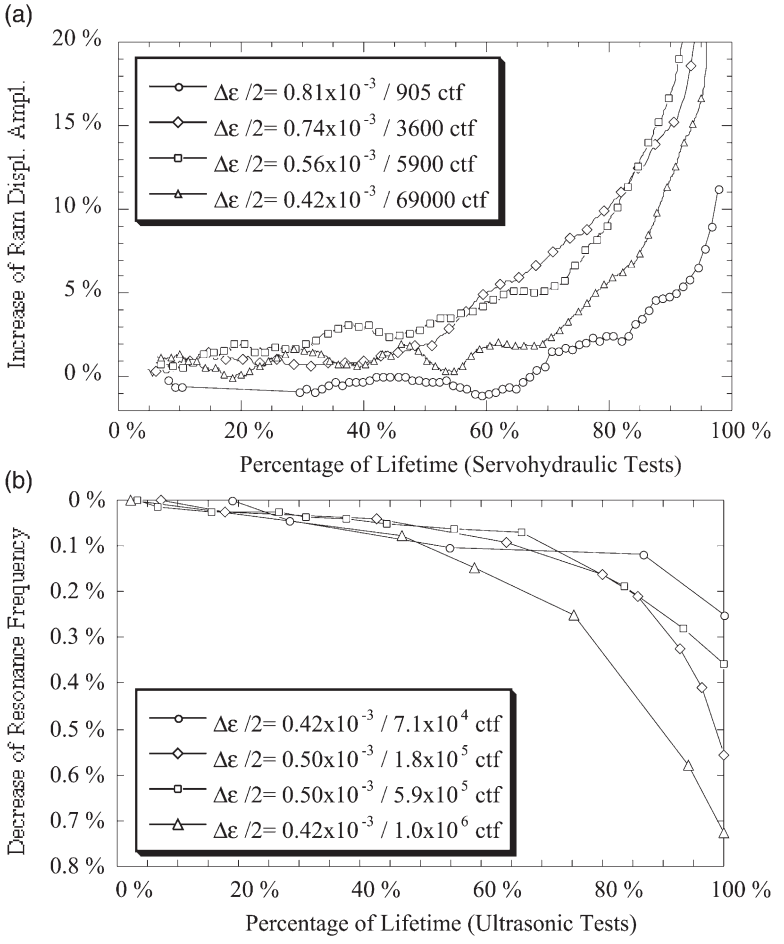

Fig. 8. Increase of ram displacement amplitude in conventional fatigue tests (a) and decrease of resonance frequency in ultrasonic fatigue tests (b). Numbers of load amplitudes are normalized with respect to cycles to failure (ctf).

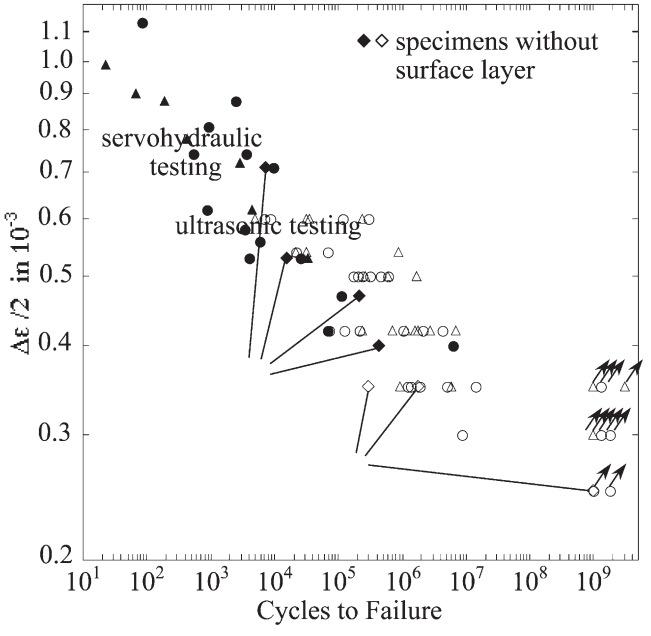

Fig. 9. Fatigue data of AlSi1Mg0.6 foam with and without surface layer (rhombohedra). Other symbols refer to Fig. 4.

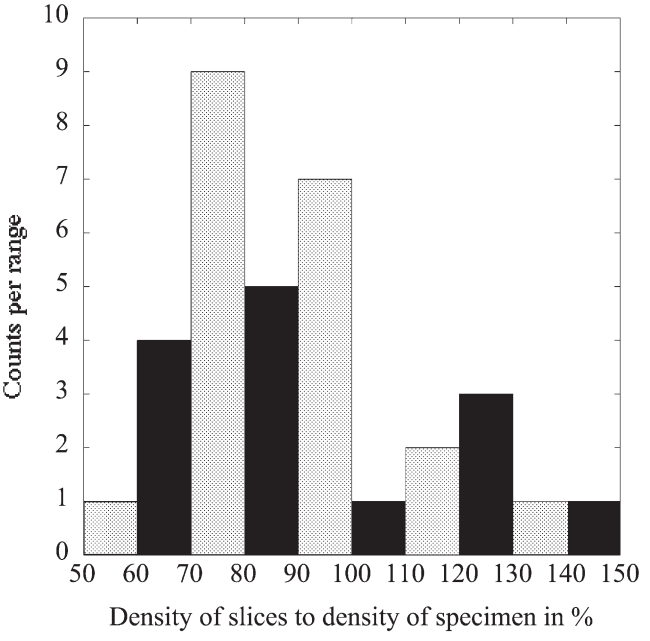

Fig. 10. Relative material density of slices (approximately 6 mm) at the place where a fatigue crack caused final fracture.

0.89±0.22. This means that no statistically significant correlation between crack initiation area and mean relative density at this place could be found in this investigation.

5. Discussion

Cyclic properties of AlMg1Si0.6 foam have been investigated with conventional and ultrasonic fatigue testing equipment. At cyclic strain amplitudes between 0.4×10^{-3} and 0.6×10^{-3}, fatigue experiments have been performed using both testing procedures. Fig. 4 shows that both sets of endurance data can be approximated with power law functions, and the exponents coincide within 10%. Scatter range of measured lifetimes determined at 1 or 10 Hz and at 20 kHz overlap. This means that analogous fatigue properties for cycles to failure above 10^4 were found changing the cyclic frequency by more than three decades. Lines indicating the different fracture probabilities, however, are shifted towards lower cycles to failure in servohydraulic experiments. One reason is probably the different testing volume: the length of the rods subjected to cyclic loading was 60 mm in conventional experiments and approximately 15 mm in ultrasonic tests. A greater volume increases the probability of severe material defects and therefore may lead to lower mean lifetimes.

High cycle fatigue data of several bulk aluminium alloys did not show a frequency influence on lifetimes, if cycled with conventional or ultrasonic equipment in ambient air [13]. One reason for this is the rather small strain rate sensitivity of fcc materials [14] if cyclic plastic deformation is small. If, however, cyclic plastic deformation is large and aluminium alloys are cycled at stresses close to the yield strength, the strain rate influences the magnitude of plastic deformation and the evolution of fatigue damage [15].

Corrosive influences are of great importance for the process of fatigue damage of aluminium alloys in ambient air [16–18]. These corrosive influences are rather rapid. Hydrogen embrittlement caused by the humidity of the ambient air was found in ultrasonic experiments, if crack growth rates are small (below approximately 10^{-9} m/cycle) [19,13]. Since crack growth rates in the regime of high numbers of cycles to failure are small, air humidity may influence fatigue properties at low as well as ultrasonic frequencies.

The similarity of the fatigue data of foam at low and ultrasonic frequency also indicates that mechanical stressing is comparable in both cases. This is well in accordance with previous investigations of high frequency vibrations of foamed structures described in the literature. Modulus of elasticity derived by dynamic measurement methods has been found to be independent of the stimulation frequency over a wide range (4–16 kHz) [20]. A resonance of cells or certain areas of the foam would significantly influence the determination of the Young's modulus. Sound velocity can be found similar to bulk material as long as $\lambda/2\pi$ (λ is the acoustic wavelength) is sufficiently above cell size [21]. The ultrasonic fatigue experiments of specimens without surface layer show that the stiffness of the foam structure is sufficient to enable the conduction of ultrasonic longitudinal waves, not only in the continuous surface layer but also in the foam structure inside. At very high frequencies, however, where λ is less than the cell size of the investigated material ($f>1$ GHz for Alulight), ultrasound propagation mechanism changes, and sound waves are guided along cell walls and nodes [21].

The fracture surfaces show a tortuous crack path and a structured fracture surface with several elevations and depressions. In contrast to the damage mechanism reported for cyclic compression loading of foams [4–9], no deformation bands were found under fully reversed loading conditions. In several areas of the cross section, the foam failed due to the growth of fatigue cracks. Fatigue cracks may be distinguished from cracks formed during cooling of the melt, since both crack fronts of unloaded fatigue cracks are closed and do not show necking, whereas a gap is typical for cracks formed during cooling of the melt. Fig. 11(a) shows a side view of a fatigue crack in a cell wall. In contrast to bulk aluminium alloys, where slow fatigue cracks preferentially grow normal to the applied stress, the orientation of crack propagation may vary significantly due to local variations of cell wall thickness. Typical thicknesses of cell walls where cracks propagated were 10–50 μm, whereas most frequent wall thickness determined by image analysis is 250–500 μm [12]. Obviously, fatigue cracks preferentially grow in areas where the cell walls are thin and local cyclic strains are high. Fatigue fracture surface is relatively smooth and shows a transcrystalline fracture mode. Beside the fatal fatigue crack, several other cracks are visible in nearby cell walls which are more frequent at higher load amplitudes. Fatigue cracks preferentially initiate at holes or pre-existing cracks in the cell walls or areas where the cell walls are thin. Other areas of the fracture surface show a quasi-static fracture mode, which is formed at high cyclic stress intensities and long crack length [Fig. 11(b)].

The continuous surface layer contributes significantly to the stiffness of the foamed rods. If the surface layer is removed, the Young's modulus decreases approximately 40%. When a fatigue crack is visible in the surface layer, a pronounced increase in the motion of the hydraulic ram or a decrease in the resonance frequency is found. However, ultrasonic fatigue experiments show a continuous decrease of the resonance frequency already from the beginning before a fatigue crack is observed in the surface layer. At constant temperature, decrease of resonance frequency in ultrasonic experiments may be attri-

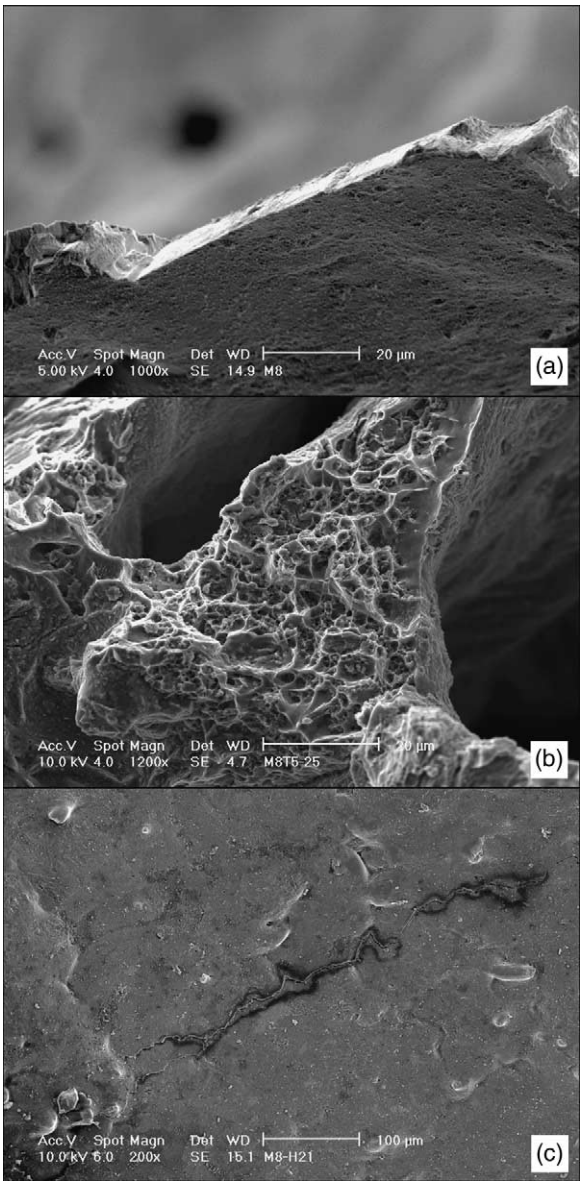

Fig. 11. Fracture surfaces of aluminium foam: smooth and transcrystalline fatigue crack growth in a cell wall (a), quasi-static fracture mode at long crack length (b), fatigue crack in a cell wall of a specimen which did not fail (c).

buted to either cyclic softening of the specimen or to the initiation of a fatigue crack. If a specimen shows cyclic softening, dissipated heat increases with increasing numbers of cycles, which was not observed. This means that the decrease in resonance frequency is caused by the formation of fatigue cracks, which start to grow from the beginning of fatigue loading already. Specimens which were cycled at the endurance limit and did not fail, showed a decreasing resonance frequency until numbers of cycles in the range of 10^6 were reached. At higher numbers of cycles, the resonance frequency remained constant. This means that cracks can initiate at the fatigue limit, however, they do not grow until final failure. Several runouts were cut into pieces and examined with the SEM. Fig. 11(c) shows as an example a cell wall in a specimen which was cycled at strain amplitude of 0.35×10^{-3} and which did not fail within 10^9 cycles. A fatigue crack with a length of approximately 600 µm is visible in a cell wall. Other specimens subjected to 10^9 cycles without failure showed that cracks in cell walls might reach maximum lengths of 3 mm [10]. These cracks are trapped when the crack tip reaches a region of greater material thickness near nodes of cells.

The process of fatigue damage of a specimen consists of two periods, i.e. the formation of fatigue cracks in cell walls in the closed cell structure followed by fracture of the surface layer. The compliance of a specimen significantly increases when approximately 60–80% of the lifetime is reached, which is mainly caused by cracking of the surface layer. Specimens without surface layer should fail at approximately 20–40% lower numbers of cycles therefore. However, the scatter of lifetimes, which is more than one decade, does not allow for distinguishing such small variations, and removing the surface layer did not show a statistically significant influence on fatigue lifetimes, if cycles to failure are plotted versus the cyclic strain. If the stress amplitude would be used to represent cyclic loading, the fatigue strength of specimens without skin would be significantly lower since the stiffness of a specimen without a surface layer is approximately only 60% of that of a foamed rod.

6. Conclusions

The cyclic properties of AlMg1Si0.6 foamed rods have been investigated with conventional fatigue testing equipment and cyclic frequencies of 1–10 Hz, and with ultrasonic fatigue testing equipment and a cyclic frequency of 20 kHz. Specimens were subjected to fully reversed loading conditions.

- Endurance data above approximately 10^4 cycles to failure obtained with servohydraulic and ultrasonic equipment coincide within the range of scatter. Similar fatigue properties were found changing the cyclic frequency more than three decades.
- Below approximately 10^7 cycles, lifetimes depend on the strain amplitudes according to a power law function.
- AlMg1Si0.6 foam shows an endurance limit. Maximum number of cycles to failure testing 73 specimens was 1.37×10^7. Specimens, which did not fail within this range also survived 10^9 cycles or more. A probability of 50% for fracture (mean endurance limit) was found at $\Delta\varepsilon/2=0.32\times10^{-3}$.
- The process of fatigue damage consists of two periods, i.e. the formation of fatigue cracks in cell walls in the closed cell structure followed by cracking of the surface layer. Preferential sites for crack initiation

are holes or pre-existing cracks in the cell walls or areas where the cell walls are thin. At the endurance limit, fatigue cracks may initiate in cell walls; however, they are trapped at nodes of cells.

- Young's modulus obtained from quasi-static experiments and with a dynamic resonance method at 20 kHz are similar (4.3±0.7 GPa and 3.9±0.7 GPa, respectively). Using this Young's modulus, the mean endurance limit is 1.31 MPa.

Acknowledgements

The authors thank the "Fonds zur Förderung der wissenschaftlichen Forschung (FWF)", Vienna for financial support of this work (project no. P1323OPHY) and the LKR-Center of Competence on Light Metals, Ranshofen, Austria for supplying the Alulight material and grant through the K-plus project.

References

[1] Haberling C, Haldenwanger H-G. Leichtbau durch lokales Aussteifen van Strukturteilen im PKW-Bau. Materialwissenschaft-und-Werkstofftechnik 2000;31(6):505–10.
[2] Fugati A, Lorenzini L. Aluminium foam for automotive application. In: Proceedings of Metal Foams and Porous Metal Structures, Bremen, Germany. Bremen: MIT Publishing, 1999:5–12.
[3] Evans AG, Hutchinson JW, Ashby MF. Multifunctionality of cellular metal systems. Prog Mater Sci 1998;43(3):171–221.
[4] Banhart J, Brinkers W. Fatigue behavior of aluminum foams. J Mater Sci Lett 1999;18(8):617–9.
[5] Olurin OB, Fleck NA, Ashby MF. Fatigue of an aluminium alloy foam. In: Proceedings of Metal Foams and Porous Metal Structures, Bremen, Germany. Bremen: MIT Publishing, 1999:365–71.
[6] Harte AM, Fleck NA, Ashby MF. Fatigue failure of an open cell and a closed cell aluminium alloy foam. Acta Mater 1999;47(8):2511–24.
[7] Schultz O, Lingeris AD, Haider O, Starke P. Fatigue behaviour, strenght and failure of aluminium foam. In: Proceedings of Metal Foams and Porous Metal Structures, Bremen, Germany. Bremen: MIT Publishing, 1999:379–86.
[8] Sugimura Y, Rabiei A, Evans AG, Harte AM, Fleck NA. Compression fatigue of a cellular Al alloy. Mater Sci Engng 1999;A269(1-2):38–48.
[9] Ashby MF, Evans AG, Fleck NA, Gibson LJ, Hutchinson JW, Wadley HNG. Metal foams: a design guide. Oxford, UK: Butterworth-Heinemann, 2000.
[10] Zettl B, Mayer H, Stanzl-Tschegg SE, Degischer HP. Fatigue properties of aluminium foams at high numbers of cycles. Mater Sci Engng 2000;A229(1):1–7.
[11] Mayer H. Fatigue crack growth and threshold measurements at very high frequencies. Int Mater Rev 1999;44(1):1–36.
[12] Degischer HP, Kriszt B. Structural investigations of Al-foam using quantitative image analysis. Vienna: Institute for Material Science, University of Technology (Vorstudie Prüftechnik und Eigenschaften von Al-Schaum), 1997.
[13] Mayer H, Papakyriacou M, Pippan R, Stanzl-Tschegg S. Influence of loading frequency on the high cycle properties of AlZnMgCu1.5 aluminium alloy. Mater Sci Engng, in press.
[14] Laird C, Charsley P. Strain rate sensitivity effects in cyclic deformation and fatigue fracture. In: Wells JM, Buck O, Roth LD, Tien JK, editors. Ultrasonic fatigue. Philadelphia: The Metallalurgical Society of AIME, 1982:187–205.
[15] Benson DK, Hancock JR. The effect of strain rate on the cyclic response of metals. Metall Trans 1974;5:1711–5.
[16] Wei RP. Some aspects of environment-enhanced fatigue-crack growth. Engng Fract Mech 1970;1:633–51.
[17] Verkin BI, Grinberg NM. The effect of vacuum on the fatigue behaviour of metals and alloys. Mater Sci Engng 1979;41:149–81.
[18] Böhmer M, Munz D. Das Dauerschwingverhalten metallischer Werkstoffe in Vakuum und in verschiedenen Gasatmosphären, Teil I. Metallwiss Techn 1970;24(5):446–55.
[19] Stanzl-Tschegg SE, Mayer HR, Tschegg EK. The influence of air humidity on near-threshold fatigue crack growth of 2024-T3 aluminium alloy. Mater Sci Engng 1991;A147:45–54.
[20] Mepura. Alulight — product information folder, A-5282. Austria: Ranshofen, 1996.
[21] Weaver R. Ultrasonics in an aluminum foam. Ultrasonics 1998;36:435–42.